0026-895X/09/7604-861–871$20.00
MOLECULAR PHARMACOLOGY
Copyright © 2009 The American Society for Pharmacology and Experimental Therapeutics
Mol Pharmacol 76:861–871, 2009

Vol. 76, No. 4
55863/3516895
Printed in U.S.A.

Novel Molecular Determinants in the Pore Region of Sodium Channels Regulate Local Anesthetic Binding

Toshio Yamagishi, Wei Xiong, Andre Kondratiev, Patricio Vélez, Ailsa Méndez-Fitzwilliam, Jeffrey R. Balser, Eduardo Marbán, and Gordon F. Tomaselli

Division of Cardiology, Department of Medicine, The Johns Hopkins University School of Medicine, Baltimore, Maryland (T.Y., W.X., A.K., P.V., A.M.-F., E.M., G.F.T.); and Departments of Pharmacology and Anesthesia, Vanderbilt University, Nashville, Tennessee (J.R.B.)

Received February 25, 2009; accepted June 26, 2009

ABSTRACT

The pore of the Na^+ channel is lined by asymmetric loops formed by the linkers between the fifth and sixth transmembrane segments (S5-S6). We investigated the role of the N-terminal portion (SS1) of the S5-S6 linkers in channel gating and local anesthetic (LA) block using site-directed cysteine mutagenesis of the rat skeletal muscle ($Na_V1.4$) channel. The mutants examined have variable effects on voltage dependence and kinetics of fast inactivation. Of the cysteine mutants immediately N-terminal to the putative DEKA selectivity filter in four domains, only Q399C in domain I and F1236C in domain III exhibit reduced use-dependent block. These two mutations also markedly accelerated the recovery from use-dependent block. Moreover, F1236C and Q399C significantly decreased the affinity of QX-314 for binding to its channel receptor by 8.5- and 3.3-fold, respectively. Oddly enough, F1236C enhanced stabilization of slow inactivation by both hastening entry into and delaying recovery from slow inactivation states. It is noteworthy that symmetric applications of QX-314 on both external and internal sides of F1236C mutant channels reduced recovery from use-dependent block, indicating an allosteric effect of external QX-314 binding on the recovery of availability of F1236C. These observations suggest that cysteine mutation in the SS1 region, particularly immediate adjacent to the DEKA ring, may lead to a structural rearrangement that alters binding of permanently charged QX-314 to its receptor. The results lend further support for a role for the selectivity filter region as a structural determinant for local anesthetic block.

Sodium channels are transmembrane proteins that rapidly conduct electrical impulses throughout nerve and muscle. The channels have a modular structure, with distinct regions mediating gating and permeation. The pore-lining (P) segments, formed by the S5-S6 linkers, are the major determinants for selective ion flux, whereas the S4 transmembrane domain and the cytoplasmic III-IV interdomain linker figure prominently in activation and fast inactivation gating, respectively. The structural separation of function is not clear-cut; mutations in the P segments are known to alter gating (Tomaselli et al., 1995; Balser et al., 1996a; Todt et al., 1999; Hilber et al., 2001; Xiong et al., 2003, 2006; Sasaki et al., 2004; Tsang et al., 2005); conversely, changes in inactivation induced by mutagenesis or toxins may alter conductance or selectivity (Wasserstrom et al., 1993a,b).

Clinically important local anesthetic drugs act by blocking ionic flux through the Na^+ channel in a conformation-specific fashion (Courtney, 1975; Hille, 1977; Hondeghem and Katzung, 1977; Starmer et al., 1984; Balser et al., 1996b), implying an important interaction between voltage-dependent gating and drug action. Site-directed mutagenesis has implicated the S6 transmembrane segment in the fourth domain (IVS6) of the Na^+ channel as a site for local anesthetic drug binding. Mutations of seven amino acids in the IV-S6 segment reduce or eliminate local anesthetic (LA) block in response to repeated stimulation, referred to as use-dependent block (Ragsdale et al., 1994). Two aromatic residues, Tyr1586 and Phe1579 in IVS6 (equivalent of Tyr1771 and Phe1764 in $rNa_V1.2$), are the critical determinants of high-affinity binding of local anesthetics to the inactivated Na^+ channels (Ragsdale et al., 1994; Qu et al., 1995; Ragsdale et al., 1996; McNulty et al., 2007; Ahern et al., 2008; Muroi and Chanda, 2009). Further recent data

The work was supported by the National Institutes of Health National Heart, Lung, and Blood Institute [Grants R01-HL50411, R01-HL52768] (to G.F.T. and E.M., respectively). G.F.T. is the Michel Mirowski Professor of Cardiology at Johns Hopkins.

T.Y. and W.X. contributed equally to this work.

Article, publication date, and citation information can be found at http://molpharm.aspetjournals.org.
doi:10.1124/mol.109.055863.

ABBREVIATIONS: P segment, pore-lining segment; LA, local anesthetic; QX-314, *N*-(2,6-dimethylphenylcarbamoylmethyl)triethylammonium bromide; MTS, methanethiosulfonate; WT, wild type.

examining block of the F1579A mutant channel by QX-314 suggest that LA drugs modulate voltage sensing of the S4 gating apparatus of the channel (Muroi and Chanda, 2009).

The P segments of the Na^+ channel have also been implicated in local anesthetic binding. Quaternary ammonium local anesthetic binding remains voltage-dependent in channels that have had inactivation gating removed chemically (Gingrich et al., 1993) or genetically consistent with drug binding in the channel pore. The fractional electrical distance for local anesthetic drug binding in the pore of the Na^+ channel has been predicted to lie ~30% into the electrical field from the extracellular surface (Strichartz, 1973; Gingrich et al., 1993; Zamponi et al., 1993a; Yamagishi et al., 1997). This places the binding site near the selectivity filter (Heinemann et al., 1992; Chiamvimonvat et al., 1996; Favre et al., 1996; Yamagishi et al., 1997). Quaternary ammonium local anesthetics such as QX-314 and QX-222 do not block skeletal muscle Na^+ channels when applied from the extracellular side. However, mutation of the selectivity filter residues D400A (domain I), E755A (domain II), and A1529D (domain IV) facilitated block by externally applied QX-314 and QX-222 and enhanced recovery from block by internal QX314. Moreover, the $rNa_V1.4$ domain I P-loop mutation, Y401C, permitted external QX-222 block (Sunami et al., 2000). These data indicate the involvement of the selectivity filter in local anesthetic binding and its proximity to the IV-S6 local anesthetic binding site (Sunami et al., 1997). Computational models of LA binding to sodium channels were also developed for docking the LA between the selectivity filter and S6 (Lipkind and Fozzard, 2005; Bruhova et al., 2008).

In this context, the present study seeks to define the role of the P segments in gating and local anesthetic block. Because QX-314 is not membrane-permeant and does not block Na^+ channels from the extracellular side, the permanently charged lidocaine derivative QX-314 was employed in an attempt to simplify drug block and focus on the effect of the P segments in pore binding of local anesthetics. The residues on the amino terminal side of the selectivity filter ring in each of the four domains were replaced with cysteine. We were particularly interested in the amino acid residues immediately N-terminal to the DEKA ring because of their structural proximity. The mutations in the SS1 region have disparate effects on the voltage dependence and kinetics of fast inactivation. F1236C and Q399C significantly attenuated the use-dependent block and accelerated recovery from use-dependent block. Marked reduction in the affinity of QX-314 for binding to its channel receptor was revealed in these mutant channels. We proposed that cysteine mutations in the SS1 region, particularly immediate adjacent to the DEKA ring, may lead to a structural rearrangement that alters the binding of permanently charged QX-314 to its receptor. These new molecular determinants in the selectivity filter region are implicated in local anesthetic block.

Materials and Methods

Mutagenesis and Channel Expression. Mutagenesis and transformation of the expression plasmid containing the rat skeletal muscle (μ1) α subunit of the Na^+ channel was performed as described previously (Yamagishi et al., 1997). The wild-type μl Na^+ channel cDNA (Trimmer et al., 1989) was cloned into the mammalian expression vector pGW1H (BD Biosciences, Oxford, UK) for both mutagenesis and expression in tsA-201 cells. The rat brain β1 subunit (Isom et al., 1992) was cloned into pCMV-5. A plasmid containing the green fluorescent protein (pGreenLantern; Invitrogen, Carlsbad, CA) was used as a transfection reporter.

Cysteine substitutions were introduced into the rat μ1 skeletal muscle channel α subunit by oligonucleotide-directed mutagenesis as described previously (Pérez-García et al., 1996) or by polymerase chain reaction with overlapping mutagenic primers (QuikChange site-directed mutagenesis kit; Stratagene, La Jolla, CA). All mutations were performed in duplicate and confirmed by DNA sequencing.

TsA-201 cells, a transformed human embryonic kidney 293 cell line expressing the Simian virus 40 T-antigen, were used for channel expression. The culture and transfection conditions were as described previously (Yamagishi et al., 1997). Transfection was performed by the calcium phosphate precipitation method for 6 to 12 h with a combination of 2.5 μg of the wild-type or mutant α subunit, 1 μg of the β1 subunit, and 0.3 μg of the green fluorescent protein cDNA-containing plasmids per 35-mm dish.

Electrophysiology. Transfected cells were identified by epifluorescence microscopy and voltage-clamped using the whole-cell configuration of the patch-clamp technique (Hamill et al., 1981) 24 to 72 h after transfection. Cells were transferred to the stage of an inverted microscope and superfused with bath solution (see below) at a rate of 1 to 2 ml/min. All experiments were performed at room temperature (22–23°C). Patch electrodes were pulled from borosilicate glass and had 2 to 5 MΩ tip resistances. Cells were not used if the series resistance was higher than 6 MΩ. Currents were recorded using an Axopatch 200A patch-clamp amplifier (Molecular Devices, Sunnyvale, CA) interfaced to a personal computer. Voltage commands were issued and data collected with custom-written software. Cell capacitance was calculated by integrating the area under an uncompensated capacity transient elicited by a 20 mV hyperpolarizing test pulse from a holding potential of −80 mV. Series resistance was then compensated as much as possible without oscillations, typically 70 to 90%. Given the average series resistance of our electrodes, the maximal uncompensated voltage error was < 6 mV for the largest currents studied.

Whole-cell currents were recorded in a bath solution containing 140 mM NaCl, 5 mM KCl, 2 mM $CaCl_2$, 1 mM $MgCl_2$, 10 mM HEPES, and 10 mM glucose, pH 7.4. The pipette solution consisted of 35 mM NaCl, 105 mM CsF, 1 mM $MgCl_2$, 10 mM HEPES, and 10 mM EGTA, pH 7.2. QX-314 (Alomone Labs, Jerusalem, Israel) was added to the pipette and bath solutions at the indicated concentrations (25 μM–1 mM). All experiments were performed 5 to 15 min after establishment of the whole-cell configuration. This ensured adequate dialysis of the cell and enabled attainment of a new pseudo-steady state after the rapid phase of the well known hyperpolarizing shift of inactivation (Yamagishi et al., 1997). Peak conductance (G) was calculated by dividing peak Na^+ current by the driving force ($V - V_{rev}$), where V is the test potential and V_{rev} is the reversal potential. Activation curves were fit to the Boltzmann equation: $G/G_{max} = 1/[1 + \exp(-(V-V_{1/2})/k)]$, where G_{max} is the maximal conductance, $V_{1/2}$ is the voltage for half-activation, and k is the slope factor. After induction of steady-state inactivation by 500-ms prepulses from a holding potential of −100 mV, peak Na^+ currents were measured with 20-ms test pulses to −10 mV applied every. The steady-state inactivation curves were fit to the following Boltzmann equation: $I/I_{max} = 1/[1 + \exp((V_p - V'_{1/2})/k')]$, where I_{max} is the maximal peak current, V_p is the prepulse voltage, $V'_{1/2}$ is the voltage for half-inactivation, and k' is the slope factor.

Paired experiments were performed on wild-type and mutant channels in the presence and absence of drug. The development of use-dependent block was assayed by repeated pulsing to a test potential of −10 mV for 20 ms at different frequencies until a steady level of current reduction was achieved; the data shown were obtained at 1 Hz. Recovery from use-dependent block was assessed by

the delivery of 20-ms test pulses from a holding potential of −100 mV to −10 mV at 0.5, 1, 2, 5, 10, and 15 min after a train of rapid depolarizations to induce use-dependent block. The time course of recovery was determined by plotting the current amplitude of the test pulse normalized to the current amplitude before the induction of use-dependent block fit by a single exponential. The fractional current after 15 min at a holding potential of −100 mV is a model independent index of recovery from drug block. Half-blocking concentrations of the current by QX-314 at 1 Hz stimulation after reaching steady-state were determined by least-squares fits of the dose-response curves to a single binding site isotherm of the form: $I_{\text{first-pulse}}/I_{\text{steady-state}} = 1/\{1 + ([\text{QX-314}]/\text{IC}_{50})\}$.

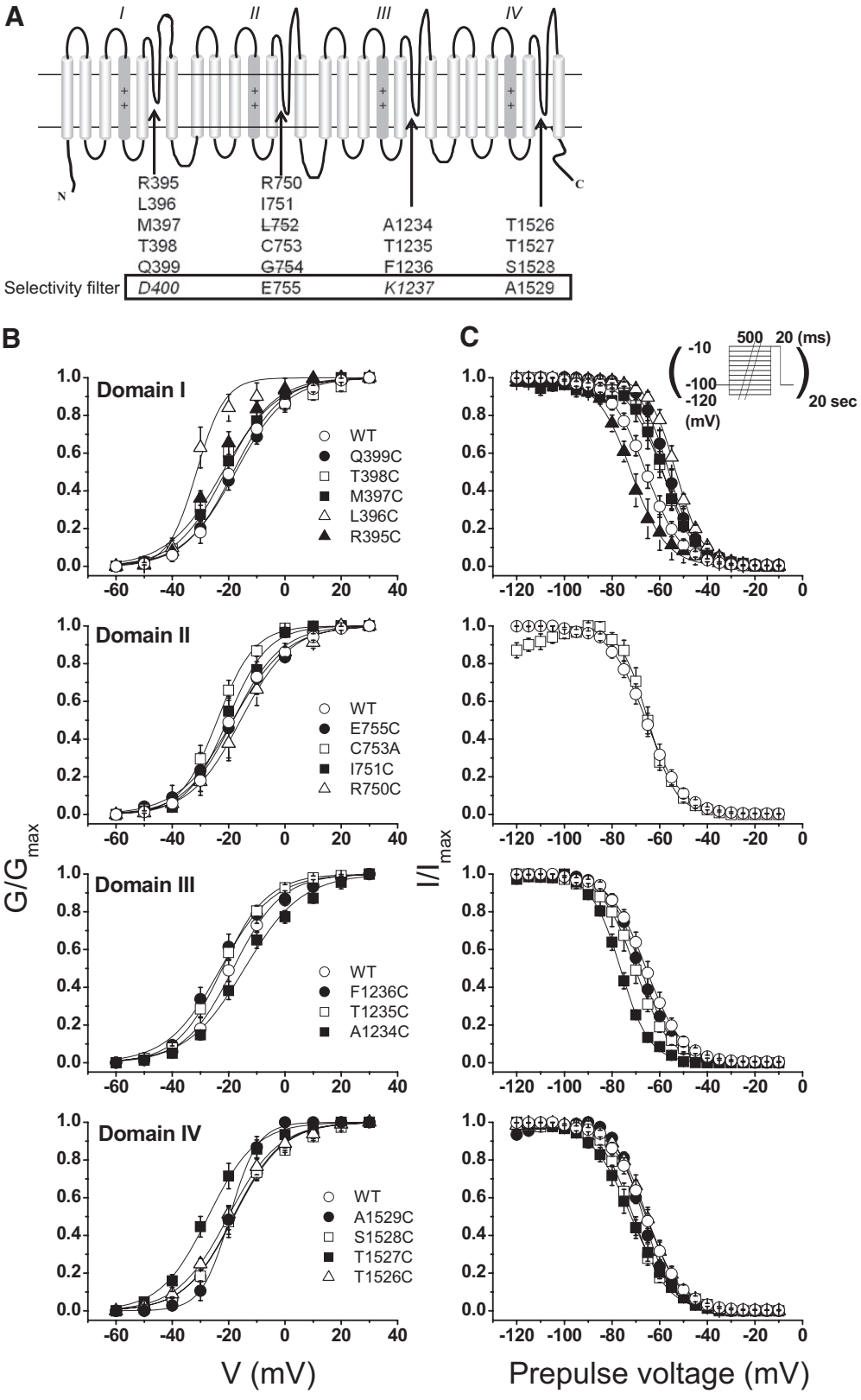

Fig. 1. A, transmembrane topology of the Na^+ channel. Arrows indicated the P segments, the regions between the fifth and sixth membrane spanning repeats. The residues that were mutated are proximal to the selectivity filter and are shown below the topology cartoon. The putative selectivity residues Asp400, Glu755, Lys1237, and A1529 are enclosed in the box. Cysteine mutants at all positions except Asp400 and Lys1237 (both in italic) were examined. Gly754 and Leu752 are labeled with a strikethrough due to nonexpression of cysteine mutants. B and C, normalized activation curves (B) and steady-state inactivation curves (C) for the wild-type and domain I-IV mutants. The solid curves are fits to a Boltzmann function as described under *Materials and Methods*. The parameters of the fits are summarized in Table 1.

Data Analysis. Pooled data are presented as means ± S.E.M. Statistical comparisons were made using analysis of variance. $p < 0.05$ was considered significant.

Results

Fig. 1A shows a schematic of the areas of the channel investigated in this study. Using the putative selectivity filter positions in each domain (Asp400, Glu755, Lys1237, and Ala1529) as landmarks, we replaced three to five residues proximal (i.e., amino-terminal) to each of these sites with cysteine. A naturally occurring cysteine in the second domain (Cys753) was mutated to alanine. All but 2 of the 17 mutants expressed Na^+-selective currents. None of the functional mutants appreciably altered the reversal potential under our experimental conditions, arguing against major changes in selectivity. Two mutations in domain II, L752C and G754C, did not express functional channels in the wild-type channel background or when C753A was used as the background for mutagenesis. As a further means of excluding the possibility that an internal disulfide bond had formed spontaneously to cripple these mutants, exposure to 1 mM dithiothreitol did not reveal any functional channels (Bénitah et al., 1997).

Voltage Dependence of Activation and Inactivation. The consequences of cysteine mutagenesis in this region of the channel are unknown; thus, we first characterized the voltage dependence of activation and inactivation in wild-type and in each mutant channel. Figure 1, B and C, show activation curves (left) and steady-state inactivation curves (right), grouped by domain. The domain I mutant L396C exhibited a 16-mV hyperpolarizing shift of activation and its neighbor R395C produced a more modest shift (7 mV) in the same direction. The domain IV mutant T1527C also shifted G/G_{max} leftward by 8 mV. Figure 1C, right, the changes of steady-state inactivation were most striking and consistent in domain I, in which four consecutive positions (396–399) shifted the h_∞ positive by 7 to 12 mV. One mutant in domain III and two in domain IV produced hyperpolarizing shifts of similar magnitude (Table 1).

Kinetics of Gating. We examined the rate of recovery from fast inactivation in each of the mutants after a 20-ms depolarization to −10 mV. Both wild-type and mutant channels exhibited a small component of slowly recovering current ($\tau > 100$ ms); this component never accounted for more than 3% of the total amplitude (Fig. 2). Although several mutants altered the fast recovery component (Table 1), only four significantly shifted the overall relationship. Inspection of the recovery curves reveals a consistent slowing of the rapid phase of repriming in all the domain III mutants, with an order-of-magnitude delay in the case of A1234C. The mutant A1529C in domain IV also slowed recovery, albeit to a lesser degree.

Given the changes of gating described above, we examined alterations in the macroscopic activation or decay of current during depolarizing steps. Figure 3A shows families of ionic currents from cells expressing wild-type, L396C, or A1234C channels. L396C exhibited significant delay in macroscopic activation and inactivation compared with the wild type. Both time to peak current and the half-time of current decay increased significantly (Fig. 3 and Table 1). Conversely, A1234C revealed faster decay of macroscopic currents (Fig. 3, B and C). None of the currents exhibited a measurable non-inactivating pedestal of current as described for several mutations that cause periodic paralysis and paramyotonia (Brown, 1993; Cannon, 1997) or long QT syndrome in the cardiac Na^+ channel (Wang et al., 1996).

Use-Dependent Block of the Na^+ Channel by Internal QX314. We next determined whether any of the inactivation gating changes observed in these mutant channels influenced local anesthetic block. State-dependent local anesthetic block predicts that mutations stabilizing the inactivated state should enhance block, whereas mutants destabi-

TABLE 1
Summary of parameters of gating in P-segment mutants
Values are presented as mean ± S.E.M.

	Activation Curve		Steady-State Inactivation Curve		Recovery from Fast Inactivation (10 ms)	$T_{1/2}$ of Inactivation at 0 mV	n
	$V_{1/2}$	k	$V'_{1/2}$	K'			
	mV		*mV*			*ms*	
WT	−18.7 ± 2.1	7.8 ± 0.6	−65.6 ± 1.6	7.6 ± 0.7		0.32 ± 0.02	7
Domain I							
Q399C	−17.8 ± 2.0	8.4 ± 0.6	−56.1 ± 2.4*	6.0 ± 1.2	N.C.	0.32 ± 0.02	12
T398C	−22.7 ± 1.5	7.3 ± 0.6	−58.7 ± 1.8*	6.7 ± 0.6	N.C.	0.30 ± 0.02	11
M397C	−20.9 ± 3.8	7.4 ± 0.7	−58.8 ± 2.1*	7.7 ± 1.2	N.C.	0.31 ± 0.02	5
L396C	−34.2 ± 2.6*	3.4 ± 0.8*	−53.2 ± 2.4*	5.8 ± 0.7	N.C.	0.57 ± 0.05*	8
R395C	−25.0 ± 1.3*	7.3 ± 0.5	−71.4 ± 5.2	8.4 ± 1.3	N.C.	0.30 ± 0.04	7
Domain II							
E755C	−18.8 ± 5.3	9.0 ± 1.1	N.D.	N.D.	N.D.	0.36 ± 0.09	4
C753A	−24.0 ± 1.4	6.5 ± 0.3	−64.9 ± 1.7	5.8 ± 0.6	N.C.	0.28 ± 0.02	4
I751C	−20.3 ± 2.1	6.8 ± 0.7	N.D.	N.D.	N.D.	0.39 ± 0.06	4
R750C	−15.7 ± 3.2	8.2 ± 0.3	N.D.	N.D.	N.D.	0.34 ± 0.05	6
Domain III							
F1236C	−23.4 ± 2.4	8.2 ± 1.0	−68.0 ± 1.8	6.8 ± 0.5	Slow	0.33 ± 0.02	9
T1235C	−22.1 ± 1.4	7.6 ± 0.5	−70.1 ± 2.2	6.9 ± 0.5	Slow	0.30 ± 0.02	10
A1234C	−15.5 ± 2.1	8.9 ± 0.4	−76.5 ± 0.9*	6.2 ± 0.2	Slow	0.25 ± 0.02*	5
Domain IV							
A1529C	−19.5 ± 1.8	5.3 ± 0.3*	−66.9 ± 1.0	6.4 ± 0.5	Slow	0.28 ± 0.03	5
S1528C	−18.4 ± 2.5	7.8 ± 0.3	−71.8 ± 1.2*	7.7 ± 0.4	N.C.	0.29 ± 0.03	5
T1527C	−26.7 ± 2.6*	7.9 ± 0.7	−72.0 ± 2.0*	8.5 ± 0.3	N.C.	0.29 ± 0.04	7
T1526C	−19.9 ± 1.6	8.8 ± 0.9	−65.3 ± 1.9	7.3 ± 0.6	N.C.	0.31 ± 0.05	5

N.C., not significantly changed; N.D., not determined.
* $P < 0.05$ versus WT.

lizing this state would reduce block. Previous studies have suggested that charged amine moiety of local anesthetic drugs binds in the pore of the Na^+ channel (Strichartz, 1973; Cahalan and Almers, 1979; Gingrich et al., 1993). To study use-dependent block, the permanently charged lidocaine congener QX-314 was examined. In the absence of internal QX-314, the wild-type $Na_V1.4$ did not decrease with repeated pulses to −10 mV from a holding potential of −100 mV at a frequency of 1 Hz (Fig. 4A, ○). There was no significant run-down of the wild-type or mutant currents. In all experiments the peak current remained stable (< 15% change) for at least 20 min in the absence of drug (data not shown).

Figure 4A illustrates the development of use-dependent block of the wild-type (○) and two mutant channels (●, ■, ▲) at a stimulation frequency of 1 Hz. The steady-state level of block depended on the concentration of QX-314. At 25 and 100 μM, the fractional current at steady state was 0.36 ± 0.07 and 0.26 ± 0.02 of that of the first pulse, respectively in WT channels (Fig. 4C, IC_{50} = 19.5 ± 6 μM). The currents elicited by the first, 20th, and 60th pulse from representative experiments with 250 μM QX-314 are shown in Fig. 4B. After 1 min, the current amplitude of wild-type sodium channels was reduced to less than 10% of that of the first pulse in the train. Of the functional mutant channels, two in domain I (L396C and Q399C) and one in domain III (F1236C) exhibited significantly less steady-state block by QX-314 (Fig. 4, B and C). The fractional current through the mutant channels L396C, Q399C, and F1236C is 0.26 ± 0.09, 0.51 ± 0.06, and 0.33 ± 0.07 compared with 0.04 ± 0.02 for the wild type (Fig. 4C). The fractional current at steady state through the other mutant channels does not differ significantly from the wild type in the presence of 250 μM internal QX-314 (Fig. 4C). The rate of decay of the Q399C and F1236C currents are similar to the wild type and do not change in the presence of QX-314 (Fig. 4B; Table 2).

Recovery from QX-314 Block. The use-dependent block of the wild-type current by internal QX-314 recovers slowly and only partially over 15 min at a holding potential of −100 mV. Recovery was assessed by brief (20 ms), infrequent test pulses (30 s and 1, 2, 5, 10, and 15 min) after the induction of use-dependent block by a 1 Hz train of depolarizing steps to −10 mV. Use-dependent block develops slowly at this stimulation frequency, $\tau \sim 10$ s (Fig. 4A). Thus, recovery assayed by single infrequent voltage steps is minimally contaminated by reblock during the test pulse. After 15 min at a holding potential of −100 mV, the wild-type current was 29 ± 7% of the predrug control compared with 79 ± 15% of Q399C and 95 ± 5% of the F1236C mutant current (Fig. 5A). The fractional recoveries at the end of the 15 min interval for four of the five (L396C, T397C, M398C, and Q399C) domain I mutants and F1236C was significantly greater than the wild-type channel (Fig. 5B). The on (k_{on}) and off (k_{off}) rate constants were calculated based on a monoexponential fit of recovery curve from QX-314 block (Fig. 5A) using a single binding site model of the form: $1/\tau_{on} = k_{on}$ [QX-314] + k_{off} and $1/\tau_{off} = k_{off}$. The k_{off} values were 11.8 ± 0.9 and 3.7 ± 0.4 ms^{-1} for F1236C and Q399C, respectively, and significantly higher compared with WT (1.8 ± 0.1 ms^{-1}) ($p < 0.05$). The k_{on} values for the development of use-dependent block (Fig. 4A) were 51.5, 32.3, and 40.6 $\mu M^{-1}s^{-1}$ for WT, Gln399, and F1236C, respectively. The dissociation constants k_d ($k_d = k_{off}/k_{on}$) for F1236C and Q399C were increased to 8.5- and 3.3-fold compared with WT ($p < 0.05$) (Table 3), respectively, suggesting that these mutants immediately adjacent to the selectivity filter significantly reduce the affinity of QX-314 for its receptor.

Effect of Slow Inactivation. The protracted kinetics of slow inactivation may have an impact on the use-dependent block of local anesthetics. Does the attenuated use-dependent block observed in Q399C and F1236C mutant channel result

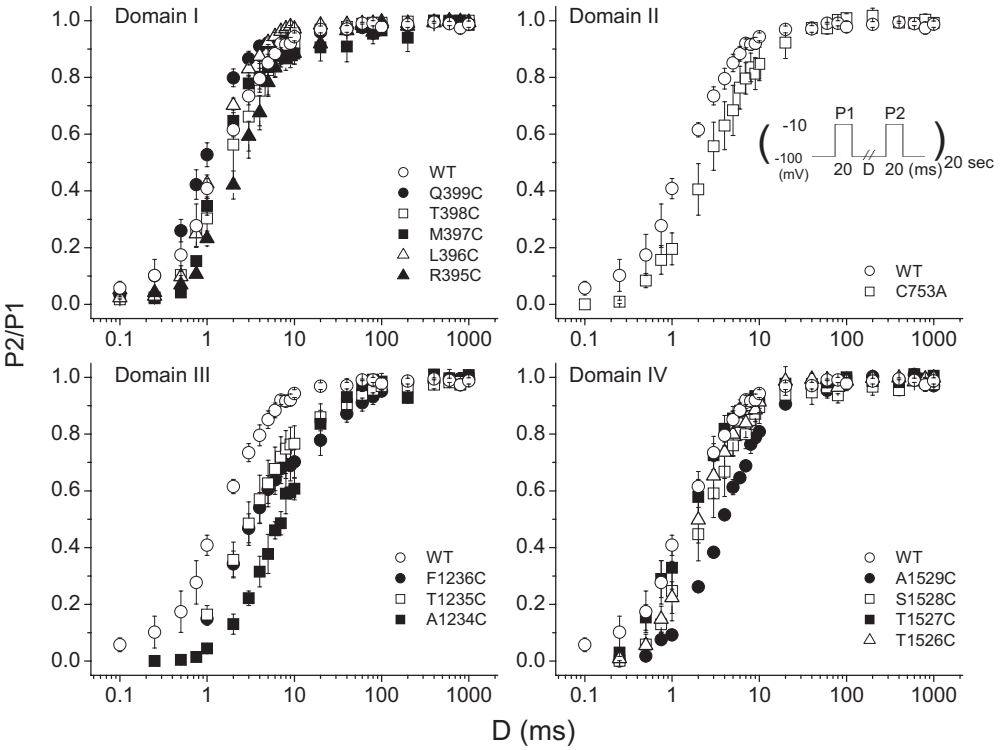

Fig. 2. Recovery of the wild-type and mutant channels. To examine recovery from fast inactivation, a paired pulse protocol was used. After a 20-ms inactivating prepulse (P1) to −10 mV, cells were recovered at −100 mV for variable test intervals. Fractional recovery (P2/P1) during the test interval was measured as the peak Na^+ current elicited by a subsequent test pulse to −10 mV (P2) relative to that measured during the prepulse (P1).

from a diminution in slow inactivation (Fig. 4)? Moreover, is the altered kinetics of macroscopic current obtained in L396C or A1234C mutant channel (Fig. 3) related to changes in slow inactivation? To address these questions, we investigated the rate of development of and recovery from slow inactivation in these mutant channels. Conditioning pulses of varying duration (3–1000 ms) to −20 mV were employed to examine the rate of entry into slow inactivated states. A 50-ms test pulse to −20 mV after 20 ms at −100 mV, to permit recovery from fast inactivation, revealed that the rate of entry into slow inactivated states was not changed in any of the mutants except F1236C. This mutant exhibited an enhanced rate of development of slow inactivation (Fig. 6A). Recovery from inactivation after a 500-ms test pulse was also uniquely slowed in F1236C (Fig. 6B).

An Allosteric Effect of External QX-314 Binding. Acceleration of recovery from QX-314 block may result from a faster unbinding rate, hastened recovery from inactivation, less efficient trapping in the pore, or an extracellular exit pathway for the drug (Ragsdale et al., 1994., 1996; Qu et al., 1995). Figure 7 plots the current amplitude over time after the addition of 1 mM QX-314 to the bath. Q399C (○) and F1236C (□) currents are not changed, but the I1575C (●) current is reduced ~30% by 0.5 mM external QX-314. The block of this mutant is similar to that observed for a mutation at the analogous position in rat brain IIA Na^+ channel, I1760A (Ragsdale et al., 1994). If an egress pathway for QX-314 to the extracellular side of the channel influences the rate of recovery, then extracellular QX-314 should delay recovery from block. Figure 7B shows the rates of recovery of the wild-type and F1236C channels in the presence of symmetrical QX-314 concentrations. External QX-314 has no effect on the recovery of the wild-type channel, L396C or Q399C in domain I mutant channels (Fig. 7C). Thus, the acceleration of recovery from use-dependent block is not the result of a mutation-induced alternative route for QX-314 to exit the pore of these domain I mutants. It is noteworthy that F1236C current is not blocked by extracellular QX-314, yet a symmetrical concentration of QX-314 slows the recovery of this mutant (Fig. 7, B and C). This may result from an allosteric effect of external QX-314 binding on the recovery of availability of F1236C.

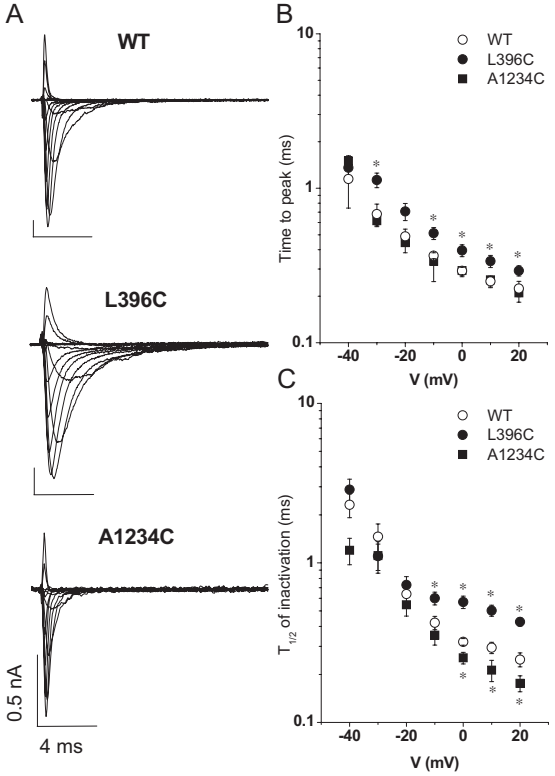

Fig. 3. A, whole-cell sodium currents of the wild-type, L396C, and A1234C mutants. The currents were elicited by depolarizations from a holding potential of −100 mV to test potentials from −50 to +60 mV in 10-mV increments. B, the times to the peak currents for wild-type, L396C, and A1234C are plotted as a function of the step voltage. C, the time from peak to 50% current decay ($t_{1/2}$) for wild-type, L396C, and A1234A is plotted as a function of the test voltage. Significant differences ($p < 0.05$) are indicated by asterisks (*).

Discussion

P-Segment Mutations and Gating Changes. The P segments of the voltage-dependent Na^+ channels are the main structural determinants of ion flux and selectivity. In addition, amino acid residues (Trp402, Glu403, Glu758, Asp1241, and Asp1532) in the P segments have been linked with slow inactivation (Tomaselli et al., 1995; Balser et al., 1996a; Xiong et al., 2003, 2006). All of these residues are carboxyl-terminal to the selectivity filter (Fig. 1), in a region of the channel that strongly influences permeation. We describe 17 mutations (including A1529C) that are amino-terminal to the selectivity filter in an area that has little effect on selectivity or conductance (Yamagishi et al., 1997). Of the 15 mutant channels that expressed, 10 exhibited a change in voltage dependence and/or kinetics. The steady-state availability curve is modestly shifted in the depolarizing direction in mutants in domain I (Q399C, T398C, M397C, and L396C), whereas one domain III mutant (A1234C) and two domain IV mutants (S1528C and T1527C) exhibit a shift in the hyperpolarizing direction. Small but statistically significant hyperpolarizing shifts in the activation curves are observed in two mutant channels in domain I (L396C and R395C) and one in domain IV (T1527C). All of the domain III mutants and A1529C in domain IV decrease the rate of recovery from fast inactivation, whereas Q399C hastens recovery. Current decay is affected in only two of the mutants, one accelerates (A1234C) and the other slows decay (L366C, Fig. 6). The fact that these properties of inactivation diverge markedly, and that they are influenced differently by mutations in the different domains, argues against a general destabilization of inactivation produced by these P-segment mutations. In fact, domain III mutants tend to stabilize inactivated states of the channel.

Use-Dependent Block by QX-314. The expressed rat skeletal muscle Na^+ channel is blocked in a use-dependent manner by QX-314 analogous to that described for expressed brain and cardiac currents (Ragsdale et al., 1994; Qu et al., 1995). The skeletal muscle channel recovers very slowly from drug block, similar to the expressed brain channel but more slowly than native or expressed cardiac Na^+ currents (Alpert et al., 1989; Baumgarten et al., 1991; Ragsdale et al., 1994; Qu et al., 1995). The use-dependent or phasic block requires channel opening, whereas the ultraslow recovery resulting from the long-lived associations of QX-314 with the Na^+ channel requires intact fast inactivation gating and trapping of the drug in its binding site (Frazier et al., 1970; Strichartz,

1973; Hille, 1977; Cahalan, 1978; Cahalan and Almers, 1979; Wang et al., 1987).

Na^+ channel mutations that generate changes in the voltage dependence of steady-state inactivation or recovery from fast inactivation might influence local anesthetic use-dependent block by altering the accessibility to the drug-binding site. The reduction in the availability of channels (Fig. 1C) results primarily from occupancy of a rapidly recovering fast-inactivated state. All of the domain I P-segment mutations except R395C shift the steady state inactivation curves in the depolarizing direction compared with the wild-type channel, indicating a destabilization of the fast-inactivated state. The depolarizing shift in the availability curve is directionally consistent with the reduction in the use-dependent block (L396C and Q399C) and enhanced recovery (L396C-T398C) from QX-314 block exhibited by these mutant channels. However, neither L396C nor Q399C significantly affected entry into or recovery from more slowly inactivating states that are associated with local anesthetic block (Balser et al., 1996b). In the absence of changes in the kinetics of recovery from slow inactivation, it is unlikely that the changes in fast-inactivation kinetics resulting from domain I P-segment mutation can account for the large differences in use-dependent QX-314 block, which are kinetically much slower.

The slow development of use-dependent block by QX-314 results from restricted access to the binding site in the channel pore. The small apparent on-rate reflects the limited access of QX-314 to the binding site during the brief period when channels are open. Accordingly, use-dependent block of both the wild-type and mutant skeletal muscle channels was hastened at faster stimulation rates (data not shown). On the other hand, recovery from use-dependent block seems to be slow and incomplete, requiring minutes to reach steady state. The mechanism underlying the slow recovery of availability is less clear. If exit of QX-314 from its binding site through an extracellular pathway is operative in accelerating recovery from block, then extracellular QX-314 should retard recovery by a mass action effect. It is noteworthy that symmetric application of QX-314 did slow recovery from internal block of F1236C. Thus, it raised the possibility that F1236C might impair the restriction imposed by the selectivity filter to allow drug access from the extracellular face of the channel. However, external application QX-314 alone did not block Na^+ current in F1236C channels. Instead, an allosteric

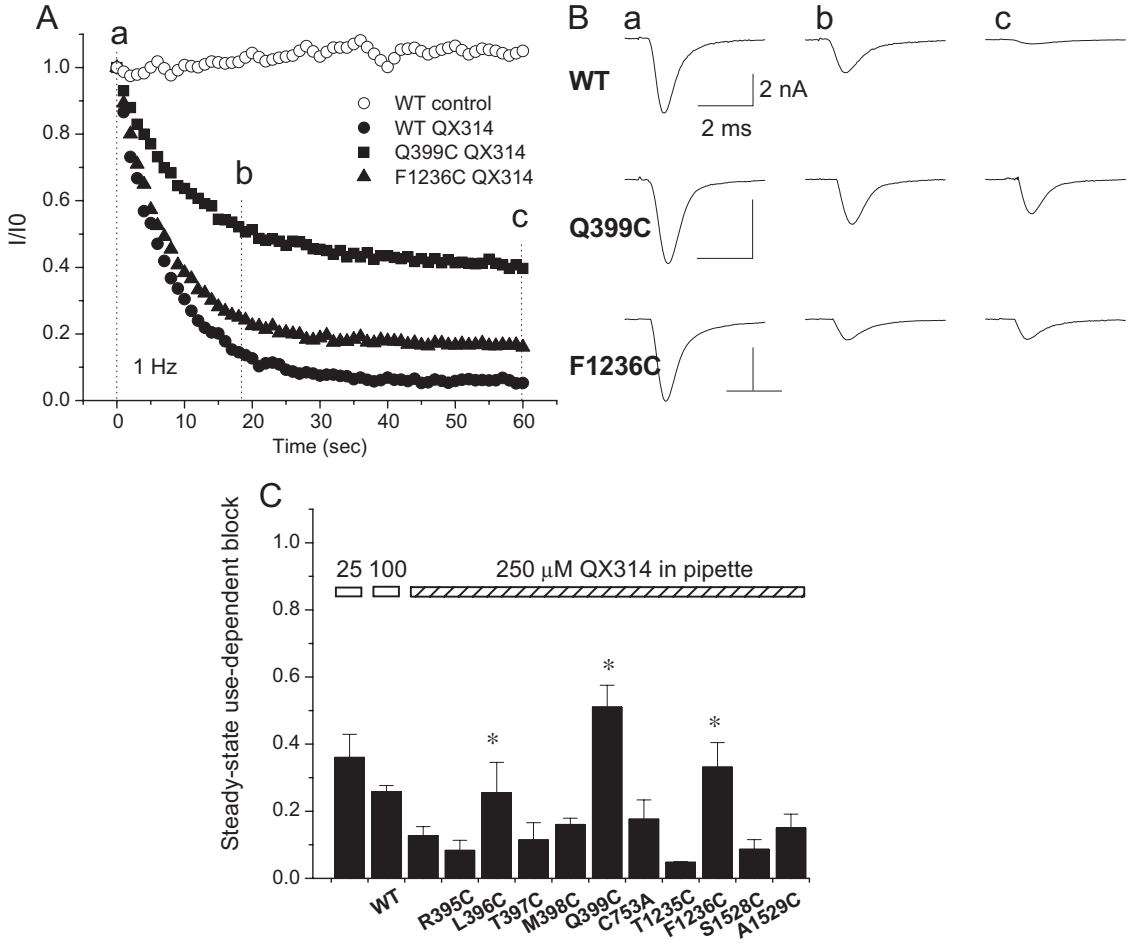

Fig. 4. A, comparison of the development of use-dependent block of Na^+ channels by 250 μM internal QX-314. Currents are elicited by voltage steps from −100 to −10 mV and normalized to the first pulse in the train for the wild-type (●, ○), Q399C (■), and F1236C (▲). B, representative whole-cell Na^+ currents in the presence of QX-314. Currents elicited by the first (a), 20th (b), and 60th (c) pulses for the wild-type, Q399C, and F1236C mutants are shown. The current amplitudes are reduced, but the time constant of current decay is not changed by QX-314. There is no significant difference in the time constant of decay between the wild type and any of the mutant channels except for L396C (see Table 2). C, bar plot of the extent of use-dependent block that develops at steady state with 250 μM QX-314 in the pipette at a stimulation frequency of 1 Hz. The height of the bars represents the fraction of current remaining at 1 min. The magnitude of use-dependent block increases with higher concentrations of QX-314. There is significantly less use-dependent block of the Q399C, L396C, and F1236C mutants ($p < 0.05$).

effect of the drug binding at an external site that affects either gating or affinity of the internal drug-binding site would be much more likely.

Residues in IV-S6 are important determinants of local anesthetic block. In $Na_V1.2$ channels, the phenylalanine at position 1764 (Phe1579 equivalent in $Na_V1.4$) and tyrosine at 1771 (Tyr1586 equivalent in $Na_V1.4$) are found to be crucial for the use-dependent block (Ragsdale et al., 1994). Mutations in this region affect both tonic and use-dependent block (Ragsdale et al., 1994, 1996; Qu et al., 1995). Phe1764 has an especially pronounced effect; mutation of this residue almost completely abolishes use-dependent block of the channel. QX-314 prominently interacts with the aromatic residue Phe1762 in $Na_V1.5$ channels (Phe1579 equivalent in $Na_V1.4$) (Qu et al., 1995). Using a series of fluorinated derivatives of aromatic amino acids (Santarelli et al., 2007), a recent study showed that cation-π interaction between lidocaine/QX-314 and π electrons of the aromatic rings of the residues only occurs for Phe1579 but not Tyr1586 (Ahern et al., 2008). The disruption of π-cation interaction of Phe1579 eliminated the use-dependent block without affecting closed-channel block. These data suggest that the positive charge in the alkylamine head of the local anesthetics is near the aromatic ring of Phe1579 during the use-dependent block (Ahern et al., 2008).

We have demonstrated that use-dependent QX-314 block of the Na^+ channel is influenced by residues in the P segments of domains I and III. The cysteine substitution mutants Q399C and L396C in domain I and F1236C in domain III reduce the steady-state level of use-dependent block by internal QX-314 (Fig. 4). Q399C and F1236C accelerate recovery from block compared with control (Fig. 5). Two other mutations in the P segment of domain I (M397C and T398C) do not alter the steady-state level of use-dependent block but enhance the extent of recovery from block (Fig. 5). The most pronounced alterations in the extent and kinetics of QX314 block seemed to be exhibited by mutations in domains I and III, which are immediately adjacent to domain IV-S6, harboring the principal local anesthetic binding site. Nevertheless, this does not necessarily exclude contribution by other domains. For example, amino acid residues of S4 (Sheets and Hanck, 2007) and S6 (Ragsdale et al., 1994; Li et al., 1999; Wang et al., 2000; Yarov-Yarovoy et al., 2001) in domains III and IV make significant contributions to use-dependent LA block, although effects of mutations in S6 of domains I and II on LA block were also observed (Nau et al., 1999; Wang et al., 2001; Yarov-Yarovoy et al., 2002; Kondratiev and Tomaselli, 2003). Moreover, a naturally occurred mutation S1710L in cardiac Na^+ channels (equivalent to Ser1528 in domain IV) reduced use-dependent block by LA (Sasaki et al., 2004).

In contrast to other mutants that only alter the kinetics of fast inactivation, F1236C stabilizes slow inactivation, which is consistent with a contribution of this mutant to slow inactivation (Ong et al., 2000; Fukuda et al., 2005). It appears paradoxical that stabilization of slow inactivation by F1236C did not directly lead to enhancement of use-dependent block; instead F1236C exhibited less use-dependent block by QX-314 (Fig. 5). It is noteworthy that F1236 is adjacent to

TABLE 2

τ_h of inactivation at −10 mV of wild-type and mutants in the absence and presence of internal QX314

Values are presented as mean ± S.E.M.

	Control		250 μM QX314	
	n	τ_h	*n*	τ_h
		ms		*ms*
WT	12	0.59 ± 0.04	6	0.66 ± 0.05
R395C	5	0.60 ± 0.06	5	0.63 ± 0.06
L396C	5	0.81* ± 0.10	5	0.83 ± 0.09
M397C	5	0.67 ± 0.10	5	0.64 ± 0.08
T398C	6	0.62 ± 0.09	6	0.71 ± 0.08
Q399C	8	0.55 ± 0.06	8	0.62 ± 0.07
C753A	5	0.59 ± 0.06	5	0.64 ± 0.08
T1235C	5	0.68 ± 0.05	4	0.66 ± 0.06
F1236C	7	0.69 ± 0.08	7	0.67 ± 0.07
S1528C	7	0.62 ± 0.04	7	0.64 ± 0.06
A1529C	5	0.69 ± 0.06	5	0.65 ± 0.09

* $P < 0.05$ verus WT in control.

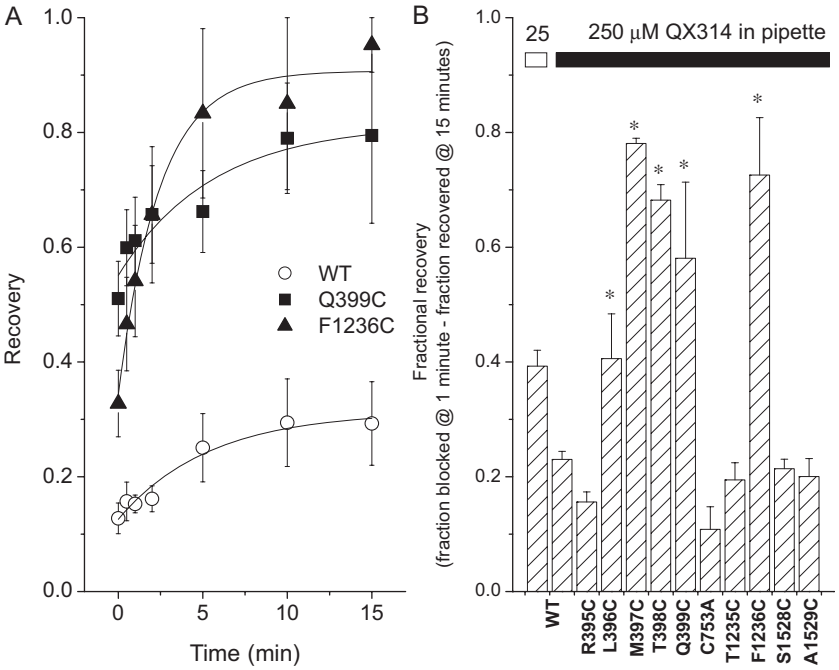

Fig. 5. A, recovery from use-dependent block is determined by depolarizing voltage steps of 20 ms delivered 30 s and 1, 5, 10, and 15 min after use-dependent block is elicited by a 60-s, 1-Hz train of depolarizations. The wild type (○), Q399C (■), and F1236C (▲) data are fit to a single exponential curve with time constants of 9.44, 4.55, and 1.41 min, respectively. The current amplitudes before the pulse train were used for normalization. B, fractional recovery of the current. For the wild-type and each of the mutants, the fractional current at 15 min of recovery minus the fraction of current remaining after a 1-Hz train of depolarizing voltage steps to elicit use-dependent block is plotted. L396C, T397C, M398C, Q399C, and F1236C exhibit significantly larger fractional recoveries at 15 min compared with the wild-type.

Lys1237, which has been linked to slow inactivation (Todt et al., 1999; Xiong et al., 2003; Szendroedi et al., 2007). Sunami et al. (1997) have demonstrated that electrostatic interactions between lidocaine binding and Lys1237, suggesting that the native lysine is located near the LA-binding site in IV-S6, and Lys1237-lidocaine predicted distance of separation is no more than 5 Å (Sunami et al., 1997). This suggests that the structural rearrangement involved in slow inactivation may move the P-loops into a position that stabilizes the interaction between the pore and QX-314, which may in turn weaken the binding (cation-π interaction) between QX-314 and Phe1579 that is critical for use-dependent block (Ahern et al., 2008). Indeed, F1236C resulted in significantly less use-dependent block by causing an 8.5-fold reduction in the affinity of binding QX-314C to its receptor (Table 3).

Implications for Local Anesthetic Drug Binding to the Na^+ Channel. Local anesthetic drug binding to the voltage-gated Na^+ channel is a complicated function of drug affinity and channel gating. QX-314 is a planar molecule with hydrophobic aromatic and positively charged quaternary amine moieties separated by 10 to 12 Å. QX-314 shares a binding site in Na^+ channels conserved across tissues and species with lidocaine and other clinically used local anesthetics (Zamponi et al., 1993a,b). The aromatic and quaternary amine regions of local anesthetics bind to different subsites on the channel. The hydrophobic subsite of LAs is composed of residues in IV-S6 (Ragsdale et al., 1994). In addition, amino acids in domain I-S6 and domain III-6 also contribute to the LA binding site (Nau et al., 1999; Yarov-Yarovoy et al., 2001, 2002). The location of the hydrophilic subsite of LA is near the selectivity filter of the channel (Sunami et al., 1997). Mutation of selectivity-filter residues change local anesthetic binding affinity, the mechanism of which is due only in part to altered electrostatic interactions between the channel and drug (Sunami et al., 1997). However, mutations of the selectivity filter often alter channel conductance and selectivity and thereby local cation concentration in the pore. Furthermore, the mutations C-terminal to the selectivity filter in the domain I P-loop or C1572T in IV-S6 create an access pathway for permanently charged local anesthetics from the extracellular space to their binding site (Sunami et al., 2000). It is noteworthy that the additive effects of these two mutants in domain I P-loop and IV-S6 suggest proximity in the 3D structure of the channel. The mutations that we describe are on the amino terminal side of the selectivity filter residues and do not exhibit differences in conductance or selectivity (Yamagishi et al., 1997). Moreover, Q399C does not alter external block of the channel by Cd^{2+} and is not accessible to MTS ethylammonium from either the extracellular or cytoplasmic surfaces. In contrast, the thiol side chain of F1236C is in the external permeation pathway, it is blocked by micromolar Cd^{2+} from the outside and is modified by MTS ethylammonium but not the larger charged reagents MTS ethyltrimethylammonium or MTS ethylsulfonate (Yamagishi et al., 1997).

The P-segment mutations Q399C and F1236C have one of

TABLE 3
On and off rates and dissociation constants of selective mutants
Values are presented as mean ± S.E.M.

	τ_{on}	τ_{off}	k_{off}	k_{on}	k_d	n
	s	min	ms^{-1}	$\mu M^{-1} \cdot s^{-1}$	μM	
WT	7.66 ± 0.72	9.44 ± 1.21	1.77 ± 0.14	51.50 ± 4.83	3.43 ± 0.40	5
Q399C	11.84 ± 0.85*	4.55 ± 0.47*	3.67 ± 0.4*2	32.31 ± 1.24*	11.35 ± 0.69*	5–10
F1236C	8.82 ± 0.91	1.41 ± 0.19*	11.78 ± 0.90*	40.61 ± 3.66	29.02 ± 3.34*	6

* $P < 0.05$ versus WT.

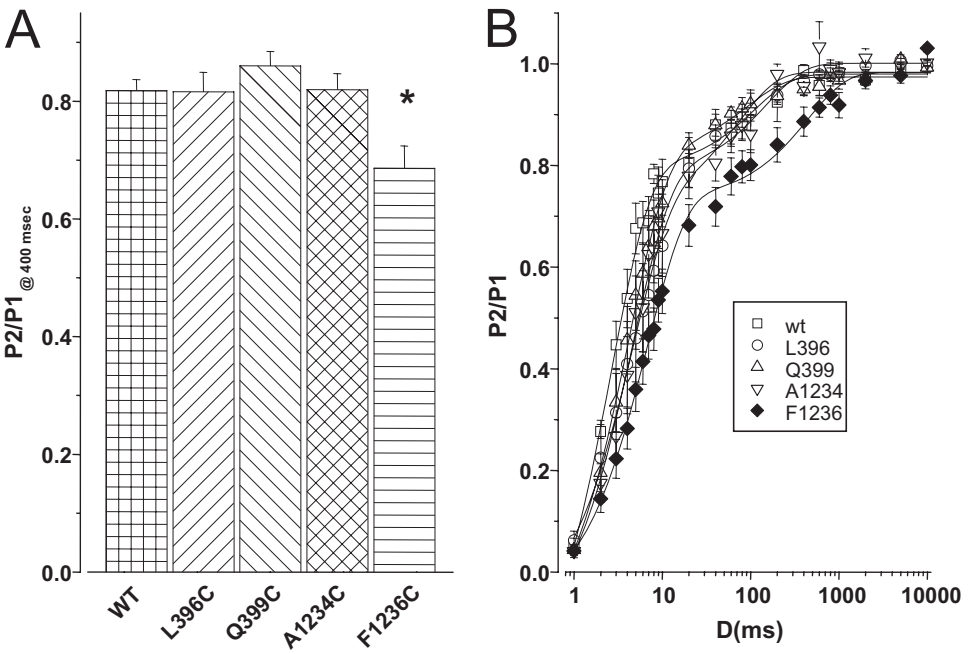

Fig. 6. Entry into and recovery from slow inactivated states. A, conditioning pulses of 3 to 1000 ms to −20 mV (P1) were used to promote entry into slow inactivated states. The rate of entry was assessed by a 50-ms test pulse to −20 mV after 20 ms at −100 mV to permit recovery from fast inactivation from a holding potential of −100 mV (P2) after the conditioning pulse. The P2/P1 ratio after a conditioning pulse duration of 400 ms is plotted. The rate of entry into slow-inactivated states was not changed in any of the mutants except F1236C (*, $p < 0.05$). B, recovery from inactivation after a 500-ms test pulse to −20 mV (P1) was assessed by a second test pulse to −20 mV (P2) after varying intervals at −100 mV. Recovery from inactivation was uniquely slowed in F1236C.

two effects on QX-314 binding: a reduction in use-dependent block or acceleration of recovery from block. An interpretation of these effects is that a local structural arrangement resulting from mutations significantly decreased the affinity (3.3- to 8.5-fold) of QX-314 for its channel receptor. These two mutants are located immediately adjacent to the charged Asp400 and Lys1237 residues of the selectivity filter. Indeed, when the size of the adjacent residue is changed, the electrostatic interaction between the charged portion of QX-314 and the putative selectivity filter DEKA would be expected. This may in turn weaken the binding (cation-π interaction) between QX-314 and Phe1579 in IV-S6. Moreover, trapping of QX-314 in the inner mouth of the channel is considered to be a major reason for the slowed recovery. Mutations that hasten this recovery may also make trapping less efficient through an effect on binding, an allosteric effect on the structure of the inner vestibule. An alternative explanation is these mutations might directly regulate LA binding, although further studies would be warranted for elucidation of detailed mechanisms.

These data highlight the importance of amino acids immediately adjacent to the selectivity filter in the SS1 region, other than IV-S6, in the block of Na channels by local anesthetics, expanding the footprint of these compounds on the cytoplasmic face of the channel.

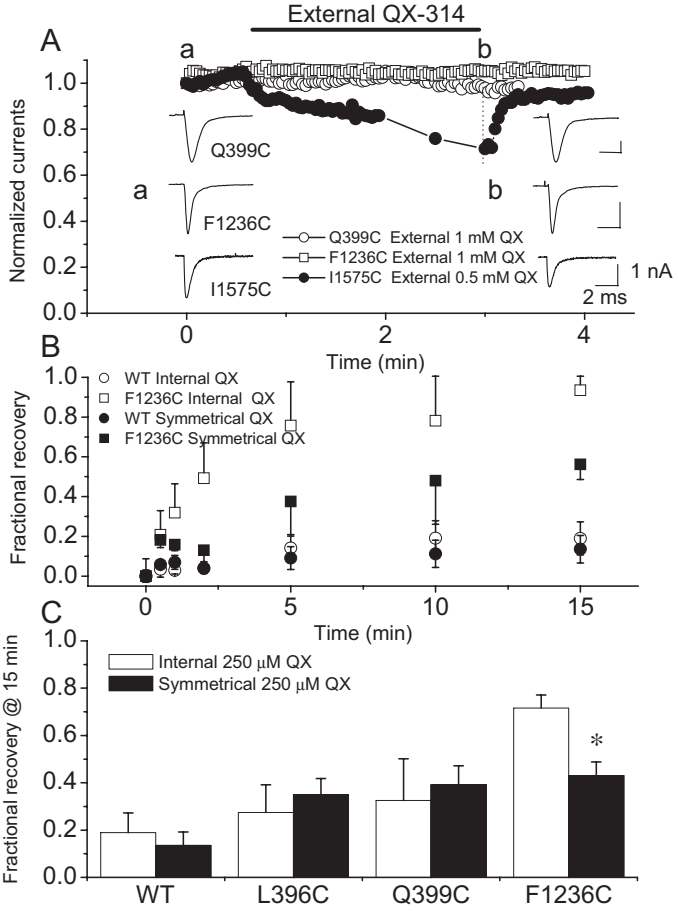

Fig. 7. External QX-314 does not block the wild-type skeletal muscle Na^+ channel or P segment mutants. A, Q399C (○) and F1236C (□) currents are elicited by depolarizing steps from −100 to −10 mV at a rate of 0.5 Hz, and 1 mM QX-314 is applied extracellularly. There is no effect on current amplitude, decay kinetics, or voltage-dependence. The I1575C (homologous to residue Ile1760 in the rat brain IIa channel) mutant in the domain IV-S6 membrane spanning repeat is blocked by ~30% by extracellular QX-314. B, recovery of the wild-type (○, ●) and F1236C (□, ■) from use-dependent block in the presence of 250 μM internal (○, □) and symmetrical (●, ■) QX-314. External QX-314 does not influence recovery of the wild-type channel but recovery of F1236C is slowed. C, symmetrical QX-314 does not significantly affect the recovery of any of the other P-segment mutants. Bar plot of the fractional recoveries with 250 mM internal (□) and symmetrical (■) QX-314.

Acknowledgments

We gratefully acknowledge Maria Janecki and Debbie DiSilvestre for technical assistance.

References

Ahern CA, Eastwood AL, Dougherty DA, and Horn R (2008) Electrostatic contributions of aromatic residues in the local anesthetic receptor of voltage-gated sodium channels. *Circ Res* **102:**86–94.

Alpert LA, Fozzard HA, Hanck DA, and Makielski JC (1989) Is there a second external lidocaine binding site on mammalian cardiac cells? *Am J Physiol* **257:** H79–H84.

Balser JR, Nuss HB, Chiamvimonvat N, Pérez-García MT, Marban E, and Tomaselli GF (1996a) External pore residue mediates slow inactivation in mu 1 rat skeletal muscle sodium channels. *J Physiol (Lond)* **494:**431–442.

Balser JR, Nuss HB, Orias DW, Johns DC, Marban E, Tomaselli GF, and Lawrence JH (1996b) Local anesthetics as effectors of allosteric gating. Lidocaine effects on inactivation-deficient rat skeletal muscle Na channels. *J Clin Invest* **98:**2874–2886.

Baumgarten CM, Makielski JC, and Fozzard HA (1991) External site for local anesthetic block of cardiac Na^+ channels. *J Mol Cell Cardiol* **23 (Suppl 1):**85–93.

Bénitah JP, Ranjan R, Yamagishi T, Janecki M, Tomaselli GF, and Marban E (1997) Molecular motions within the pore of voltage-dependent sodium channels. *Biophys J* **73:**603–613.

Brown RH Jr. (1993) Ion channel mutations in periodic paralysis and related myotonic diseases. *Ann N Y Acad Sci* **707:**305–316.

Bruhova I, Tikhonov DB, and Zhorov BS (2008) Access and binding of local anesthetics in the closed sodium channel. *Mol Pharmacol* **74:**1033–1045.

Cahalan MD (1978) Local anesthetic block of sodium channels in normal and pronase-treated squid giant axons. *Biophys J* **23:**285–311.

Cahalan MD and Almers W (1979) Interactions between quaternary lidocaine, the sodium channel gates, and tetrodotoxin. *Biophys J* **27:**39–55.

Cannon SC (1997) From mutation to myotonia in sodium channel disorders. *Neuromuscul Disord* **7:**241–249.

Chiamvimonvat N, Pérez-García MT, Ranjan R, Marban E, and Tomaselli GF (1996) Depth asymmetries of the pore-lining segments of the Na^+ channel revealed by cysteine mutagenesis. *Neuron* **16:**1037–1047.

Courtney KR (1975) Mechanism of frequency-dependent inhibition of sodium currents in frog myelinated nerve by the lidocaine derivative GEA. *J Pharmacol Exp Ther* **195:**225–236.

Favre I, Moczydlowski E, and Schild L (1996) On the structural basis for ionic selectivity among Na^+, K+, and Ca^{2+} in the voltage-gated sodium channel. *Biophys J* **71:**3110–3125.

Frazier DT, Narahashi T, and Yamada M (1970) The site of action and active form of local anesthetics. II. Experiments with quaternary compounds. *J Pharmacol Exp Ther* **171:**45–51.

Fukuda K, Nakajima T, Viswanathan PC, and Balser JR (2005) Compound-specific Na^+ channel pore conformational changes induced by local anaesthetics. *J Physiol (Lond)* **564:**21–31.

Gingrich KJ, Beardsley D, and Yue DT (1993) Ultra-deep blockade of Na^+ channels by a quaternary ammonium ion: catalysis by a transition-intermediate state? *J Physiol (Lond)* **471:**319–341.

Hamill OP, Marty A, Neher E, Sakmann B, and Sigworth FJ (1981) Improved patch-clamp techniques for high-resolution current recording from cells and cell-free membrane patches. *Pflugers Arch* **391:**85–100.

Heinemann SH, Terlau H, Stühmer W, Imoto K, and Numa S (1992) Calcium channel characteristics conferred on the sodium channel by single mutations. *Nature* **356:**441–443.

Hilber K, Sandtner W, Kudlacek O, Glaaser IW, Weisz E, Kyle JW, French RJ, Fozzard HA, Dudley SC, and Todt H (2001) The selectivity filter of the voltage-gated sodium channel is involved in channel activation. *J Biol Chem* **276:**27831–27839.

Hille B (1977) Local anesthetics: hydrophilic and hydrophobic pathways for the drug-receptor reaction. *J Gen Physiol* **69:**497–515.

Hondeghem LM and Katzung BG (1977) Time- and voltage-dependent interactions of antiarrhythmic drugs with cardiac sodium channels. *Biochim Biophys Acta* **472:** 373–398.

Isom LL, De Jongh KS, Patton DE, Reber BF, Offord J, Charbonneau H, Walsh K, Goldin AL, and Catterall WA (1992) Primary structure and functional expression of the beta 1 subunit of the rat brain sodium channel. *Science* **256:**839–842.

Kondratiev A and Tomaselli GF (2003) Altered gating and local anesthetic block mediated by residues in the I-S6 and II-S6 transmembrane segments of voltage-dependent Na^+ channels. *Mol Pharmacol* **64:**741–752.

Li HL, Galue A, Meadows L, and Ragsdale DS (1999) A molecular basis for the different local anesthetic affinities of resting versus open and inactivated states of the sodium channel. *Mol Pharmacol* **55:**134–141.

Lipkind GM and Fozzard HA (2005) Molecular modeling of local anesthetic drug binding by voltage-gated sodium channels. *Mol Pharmacol* **68:**1611–1622.

McNulty MM, Edgerton GB, Shah RD, Hanck DA, Fozzard HA, and Lipkind GM (2007) Charge at the lidocaine binding site residue Phe-1759 affects permeation in human cardiac voltage-gated sodium channels. *J Physiol (Lond)* **581:**741–755.
Muroi Y and Chanda B (2009) Local anesthetics disrupt energetic coupling between the voltage-sensing segments of a sodium channel. *J Gen Physiol* **133:**1–15.
Nau C, Wang SY, Strichartz GR, and Wang GK (1999) Point mutations at N434 in D1–S6 of mu1 Na^+ channels modulate binding affinity and stereoselectivity of local anesthetic enantiomers. *Mol Pharmacol* **56:**404–413.
Ong BH, Tomaselli GF, and Balser JR (2000) A structural rearrangement in the sodium channel pore linked to slow inactivation and use dependence. *J Gen Physiol* **116:**653–662.
Pérez-García MT, Chiamvimonvat N, Marban E, and Tomaselli GF (1996) Structure of the sodium channel pore revealed by serial cysteine mutagenesis. *Proc Natl Acad Sci U S A* **93:**300–304.
Qu Y, Rogers J, Tanada T, Scheuer T, and Catterall WA (1995) Molecular determinants of drug access to the receptor site for antiarrhythmic drugs in the cardiac Na^+ channel. *Proc Natl Acad Sci U S A* **92:**11839–11843.
Ragsdale DS, McPhee JC, Scheuer T, and Catterall WA (1994) Molecular determinants of state-dependent block of Na^+ channels by local anesthetics. *Science* **265:**1724–1728.
Ragsdale DS, McPhee JC, Scheuer T, and Catterall WA (1996) Common molecular determinants of local anesthetic, antiarrhythmic, and anticonvulsant block of voltage-gated Na^+ channels. *Proc Natl Acad Sci U S A* **93:**9270–9275.
Santarelli VP, Eastwood AL, Dougherty DA, Horn R, and Ahern CA (2007) A cation-pi interaction discriminates among sodium channels that are either sensitive or resistant to tetrodotoxin block. *J Biol Chem* **282:**8044–8051.
Sasaki K, Makita N, Sunami A, Sakurada H, Shirai N, Yokoi H, Kimura A, Tohse N, Hiraoka M, and Kitabatake A (2004) Unexpected mexiletine responses of a mutant cardiac Na^+ channel implicate the selectivity filter as a structural determinant of antiarrhythmic drug access. *Mol Pharmacol* **66:**330–336.
Sheets MF and Hanck DA (2007) Outward stabilization of the S4 segments in domains III and IV enhances lidocaine block of sodium channels. *J Physiol (Lond)* **582:**317–334.
Starmer CF, Grant AO, and Strauss HC (1984) Mechanisms of use-dependent block of sodium channels in excitable membranes by local anesthetics. *Biophys J* **46:**15–27.
Strichartz GR (1973) The inhibition of sodium currents in myelinated nerve by quaternary derivatives of lidocaine. *J Gen Physiol* **62:**37–57.
Sunami A, Dudley SC Jr, and Fozzard HA (1997) Sodium channel selectivity filter regulates antiarrhythmic drug binding. *Proc Natl Acad Sci U S A* **94:**14126–14131.
Sunami A, Glaaser IW, and Fozzard HA (2000) A critical residue for isoform difference in tetrodotoxin affinity is a molecular determinant of the external access path for local anesthetics in the cardiac sodium channel. *Proc Natl Acad Sci U S A* **97:**2326–2331.
Szendroedi J, Sandtner W, Zarrabi T, Zebedin E, Hilber K, Dudley SC, Jr., Fozzard HA, and Todt H (2007) Speeding the recovery from ultraslow inactivation of voltage-gated Na^+ channels by metal ion binding to the selectivity filter: a foot-on-the-door? *Biophys J* **93:**4209–4224.
Todt H, Dudley SC, Jr., Kyle JW, French RJ, and Fozzard HA (1999) Ultra-slow inactivation in mu1 Na^+ channels is produced by a structural rearrangement of the outer vestibule. *Biophys J* **76:**1335–1345.
Tomaselli GF, Chiamvimonvat N, Nuss HB, Balser JR, Pérez-García MT, Xu RH, Orias DW, Backx PH, and Marban E (1995) A mutation in the pore of the sodium channel alters gating. *Biophys J* **68:**1814–1827.
Trimmer JS, Cooperman SS, Tomiko SA, Zhou JY, Crean SM, Boyle MB, Kallen RG, Sheng ZH, Barchi RL, and Sigworth FJ (1989) Primary structure and functional expression of a mammalian skeletal muscle sodium channel. *Neuron* **3:**33–49.
Tsang SY, Tsushima RG, Tomaselli GF, Li RA, and Backx PH (2005) A multifunctional aromatic residue in the external pore vestibule of Na^+ channels contributes to the local anesthetic receptor. *Mol Pharmacol* **67:**424–434.
Wang DW, Yazawa K, George AL Jr, and Bennett PB (1996) Characterization of human cardiac Na^+ channel mutations in the congenital long QT syndrome. *Proc Natl Acad Sci U S A* **93:**13200–13205.
Wang GK, Brodwick MS, Eaton DC, and Strichartz GR (1987) Inhibition of sodium currents by local anesthetics in chloramine-T-treated squid axons. The role of channel activation. *J Gen Physiol* **89:**645–667.
Wang SY, Barile M, and Wang GK (2001) Disparate role of Na(+) channel D2–S6 residues in batrachotoxin and local anesthetic action. *Mol Pharmacol* **59:**1100–1107.
Wang SY, Nau C, and Wang GK (2000) Residues in Na(+) channel D3–S6 segment modulate both batrachotoxin and local anesthetic affinities. *Biophys J* **79:**1379–1387.
Wasserstrom JA, Kelly JE, and Liberty KN (1993a) Modification of cardiac Na^+ channels by anthopleurin-A: effects on gating and kinetics. *Pflugers Arch* **424:**15–24.
Wasserstrom JA, Liberty K, Kelly J, Santucci P, and Myers M (1993b) Modification of cardiac Na^+ channels by batrachotoxin: effects on gating, kinetics, and local anesthetic binding. *Biophys J* **65:**386–395.
Xiong W, Farukhi YZ, Tian Y, Disilvestre D, Li RA, and Tomaselli GF (2006) A conserved ring of charge in mammalian Na^+ channels: a molecular regulator of the outer pore conformation during slow inactivation. *J Physiol (Lond)* **576:**739–754.
Xiong W, Li RA, Tian Y, and Tomaselli GF (2003) Molecular motions of the outer ring of charge of the sodium channel: do they couple to slow inactivation? *J Gen Physiol* **122:**323–332.
Yamagishi T, Janecki M, Marban E, and Tomaselli GF (1997) Topology of the P segments in the sodium channel pore revealed by cysteine mutagenesis. *Biophys J* **73:**195–204.
Yarov-Yarovoy V, Brown J, Sharp EM, Clare JJ, Scheuer T, and Catterall WA (2001) Molecular determinants of voltage-dependent gating and binding of pore-blocking drugs in transmembrane segment IIIS6 of the Na(+) channel alpha subunit. *J Biol Chem* **276:**20–27.
Yarov-Yarovoy V, McPhee JC, Idsvoog D, Pate C, Scheuer T, and Catterall WA (2002) Role of amino acid residues in transmembrane segments IS6 and IIS6 of the Na^+ channel alpha subunit in voltage-dependent gating and drug block. *J Biol Chem* **277:**35393–35401.
Zamponi GW, Doyle DD, and French RJ (1993a) Fast lidocaine block of cardiac and skeletal muscle sodium channels: one site with two routes of access. *Biophys J* **65:**80–90.
Zamponi GW, Doyle DD, and French RJ (1993b) State-dependent block underlies the tissue specificity of lidocaine action on batrachotoxin-activated cardiac sodium channels. *Biophys J* **65:**91–100.

Address correspondence to: Dr. Gordon F. Tomaselli, Division of Cardiology, Department of Medicine, Johns Hopkins University School of Medicine, 720 Rutland Ave / Ross 844, Baltimore, MD 21205. E-mail: gtomase1@jhmi.edu